

A Novel Method to Correlate Layer Charge and the Catalytic Activity of 2:1 Dioctahedral Smectite Clays in Terms of Binding the Interlayer Cation Surrounded by Monohydrate

Abhijit Chatterjee,* Takashi Iwasaki, and Takeo Ebina

Inorganic Materials Section, Tohoku National Industrial Research Institute, 4-2-1 Nigatake, Miyagino-ku, Sendai 983-8551, Japan

Received: March 17, 2000; In Final Form: June 20, 2000

Ab initio total energy pseudopotential calculations were performed on 2:1 dioctahedral smectite to rationalize an understanding of the structure and energetics for the same and to correlate catalytic activity of clay materials with layer charge. We have chosen two clay members from the 2:1 dioctahedral smectite family—(1) beidellite and (2) montmorillonite—to monitor the effect of negative charge on the location of interlayer cation. Local softness calculation using Fukui functions generated for clusters derived from the structures of the clay matrixes in the domain of the hard-soft acid-base (HSAB) principle were performed first to locate the active site in clay. Ab initio calculations were followed to determine the most feasible orientation of the single interlayer water molecule in hydrated montmorillonite and beidellite. The role of hydroxyl hydrogen attached with the bridging oxygen connected to octahedral aluminum was also monitored. It is observed that interlayer cation (Na^+) has a lesser influence on hydrogen bond formation in the presence of single water molecule. The Na^+ locates closer to the substituted octahedral site of 2:1 dioctahedral smectite. Now, to monitor the effect of negative charge on the location of interlayer cation, the two structures chosen were compared. A novel method to correlate catalytic activity of clay with layer charge has been formulated.

Introduction

Clays are lamellar aluminosilicates showing a large variety of physicochemical properties: swelling, adsorption, ion exchange, surface acidity, etc. Now in the case of smectites the catalytic activity solely lies on the orientation of the hydroxyl hydrogen attached to the octahedral aluminum present in 2:1 dioctahedral smectite.^{1,2} Sposito et al.¹ pointed out that in case of dioctahedral clays the OH bond is directed parallel to the clay sheet with the hydrogen pointing to the octahedral vacancy. This OH may act as the active site for molecular adsorption, as proposed by Delville et al.² Since these hydroxyl groups are expected to play a major role in the catalytic activity of 2:1 clays, in their interaction with water and other polar molecules in the presence of interlayer cation, it is important to examine their orientation more closely. Interlayer cation and charged clay surfaces interact strongly with polar solvents. As a result, 2:1 clays expand in the presence of water in aqueous solution. This process is known as crystalline swelling.³ The extent of crystalline swelling is controlled by a balance between relatively strong swelling forces, due to the hydration potential of the interlayer cations and charge sites and electrostatic forces of attraction between the negatively charged 2:1 phyllosilicate layer and the positively charged interlayer cation.⁴ The structure of water and the distribution of interlayer cations at the clay–water interface remain topics of great interest in colloid science.^{5,6} There are many theoretical models to reproduce the solvent–ion–support interaction system.⁷ They either neglect the support structure assuming it as a smooth surface or the structure of solvent assuming it as continuum. A fundamental but unresolved issue is the extent to which interlayer cations determine the arrangement of interlayer water molecules in 2:1

smectite family.^{8–10} The equilibrium hydration state of a clay in the regime of integer-layer hydrates^{11,12} is known to be a function of the magnitude and location of the clay layer charge, the interlayer ion identity, the applied pressure, the temperature, and the water chemical potential as determined by vapor pressure or solution ionic strength using molecular dynamics. Many MC simulations have been directed to understand the swelling of clays or to study the clay–water interface.^{13–17} A recent experimental study probed the influence of layer charge on the hydration of the external surface of expandable 2:1 phyllosilicates.¹⁸ The model assumes that interlayer volume controls interlayer hydration and the number of cation/charge sites on external surfaces controls hydration of external surfaces.

Delville² has shown that the water molecules form a hydrogen bond with the lone pair of the oxygen at the center of the hexagonal cavity. This is possible for dioctahedral clays, since the proton is directed parallel to the plane of the clay. There are suggestions from electrostatic calculations¹⁹ that the orientations of these hydroxyl groups are sensitive to the octahedral cation plane at the center of the clay layer. In our earlier study we rationalized the structure–property relationship in montmorillonite clays.^{20–23} We observed that these hydroxyl groups expected to play a crucial role in the catalytic activity of dioctahedral clays.

Now, the hard-soft acid-base (HSAB) principles classify the interaction between acids and bases in terms of global softness. Pearson proposed the global HSAB principle.²⁴ The global hardness was defined as the second derivative of energy with respect to the number of electrons at constant temperature and external potential, which includes the nuclear field. The global softness is the inverse of this. Pearson also suggested a principle of maximum hardness (PMH),²⁵ which states that, for a constant external potential, the system with the maximum global hardness is most stable. In recent days, DFT has gained widespread use

* Corresponding author: Phone: +81-22-237-5211. Fax: +81-22-236-6839. E-mail: chatt@niri.go.jp.

in quantum chemistry. Some DFT-based local properties, e.g., Fukui functions and local softness,²⁶ have already been used for the reliable predictions in various types of electrophilic and nucleophilic reactions in the case of zeolites and clay materials.^{27–29}

In the present communication our aim is to propose a novel method to correlate layer charge and catalytic activity of 2:1 dioctahedral clay in terms of binding a single water molecule. Initially we located the active site of the clay matrixes in the domain of HSAB principle using a cluster model. This is followed by *ab initio* total energy pseudopotential calculations to rationalize the structure of the clay interlayer. Various parameters have been monitored with the *ab initio* pseudopotential calculations to propose the orientation of the interlayer cation, the stability of the water molecule inside the interlayer, and the bonding associated in that stabilization. We also monitored the influence of the interlayer cation (Na^+) in the water–clay surface interaction. We have chosen two clay members from the 2:1 dioctahedral smectite family: (1) beidellite and (2) montmorillonite. The role of hydroxyl hydrogen attached with the bridging oxygen connected to octahedral aluminum was also monitored. The novelty of the method is validated by the correlation observed based on the results of the two approaches.

Method and Model

In the present study, all cluster calculations have been carried out with DFT³⁰ using DMOL code of MSI Inc. BLYP^{31,32} exchange correlation functional and DNP basis set⁴² was used through out the calculation. The Fukui function is defined by ref 26 as follows:

$$f(r) = [\delta\mu/\delta v(r)]_N = [\delta\rho(r)/\delta N]_v \quad (1)$$

The function f is the local quantity, which has different values at different points in the species, N is the total number of electrons, μ is the chemical potential, and v is the potential acting on an electron due to all nuclei present. The theory of reactivity index calculations is mentioned elsewhere in detail.²⁷ Single-point calculations of the cation and anion of each molecule at the optimized geometry of the neutral molecule were also carried out to evaluate Fukui functions and global and local softness. The gross atomic charges were evaluated by using the technique of electrostatic potential (ESP)-driven charges. It is well-known that Mulliken charges are highly basis-set dependent, whereas ESP-driven charges show less basis-set dependence^{26,34} and are better descriptors of the molecular electronic density distribution.

The software package CASTEP (Cambridge Serial Total Energy Package), which has been described elsewhere,^{35,36} and associated programs for symmetry analysis were used for the calculations. CASTEP is a pseudopotential total energy code that employs Perdew and Zinger³⁷ parametrization of the exchange-correlation energy, supercells, and special point integration over the Brillouin zone and a plane wave basis set for the expansion of the wave functions. The methodology has been used in mineralogy to examine the hydration of corderite.³⁸ Becke-Perdew parametrization^{39,40} of the exchange-correlation functional, which includes gradient correction (GGA), was employed, as this is a well-established technique.^{41,42} The pseudopotentials are constructed from the CASTEP database. The screening effect of core electrons is approximated by LDA, while the screening effect for valence electrons is approximated by GGA. This is a reasonable approximation as shown by Garcia et al.⁴³ To obtain equilibrium structures for a given set of lattice

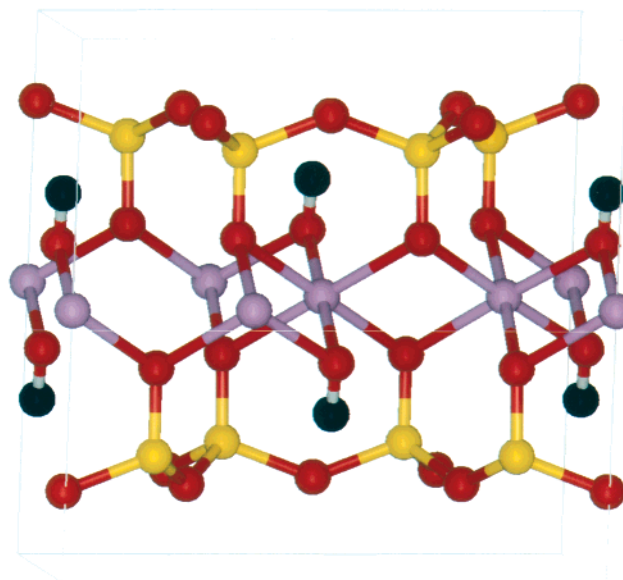


Figure 1. Structure of pyrophyllite projected onto the a – c plane. The color code is as follows: red, oxygen; yellow, silicon; magenta, octahedral aluminum; black, hydroxyl hydrogen.

constants, ionic and electronic relaxations were performed using the adiabatic or Born-Openheimer approximation, where the electronic system is always in equilibrium with the ionic system. Relaxations were continued until the total energy had converged. In the present calculations, kinetic cutoff energies between 600 and 1500 eV have been used. The Monkhorst-Pack scheme⁴⁴ was used to sample the Brillouin zone. The calculations were restricted to one special K point in the Brillouin zone, placed at (0,0,0,0,0).

The general formula of 2:1 dioctahedral smectite is $\text{Na}_x\text{[Si}_a\text{Al}_{8-a}\text{]Al}_b\text{Mg}_{4-b}\text{O}_{20}(\text{OH})_4$, where $x = (12 - a - b)$ is the layer charge, and Na^+ is the balancing interlayer cation. Montmorillonite and beidellite structure has been generated from the well-defined crystal structure of dioctahedral pyrophyllite⁴⁵ having the formula $\text{Si}_8\text{Al}_4\text{O}_{20}(\text{OH})_4$ and is shown in Figure 1. The subsequent formulas of idealized montmorillonite and beidellite are $\text{NaSi}_8\text{Al}_3\text{MgO}_{20}(\text{OH})_4$ and $\text{NaAlSi}_7\text{AlO}_{20}(\text{OH})_4$, respectively. Hydrated phase calculations were performed with the starting configuration being the minimum energy structures of the clays at the unhydrated situation. Here, in our two structures the basic difference is the location of substituent cation. In both cases the charge is balanced by a counter cation. The intralayer structure was held fixed and the interlayer spacing was increased to accommodate the water molecule. In the case of pyrophyllite, the interlayer separation was kept fixed at 9.29 Å in accord with the experimental value.⁴⁶ As there is no available experimental value for the hydrated phase of pyrophyllite, the layers were relaxed until 10.52 Å to accommodate the water molecule in combination of the reference to talc,⁴⁷ and that of a MD simulation of Boek et al.¹⁷ This is a sort of approximation as the number of water molecules is related with the humidity, and here we are not incorporating the humidity parameter into our calculation. All calculations were performed with sodium as the interlayer cation. Now for the calculation of the hydrated pyrophyllite, i.e., for both montmorillonite and beidellite the water molecule was placed between the interlayer space, with its oxygen pointing toward the hydroxyl hydrogen linked to octahedral aluminum. The orientation of water on both montmorillonite and beidellite surfaces is shown in Figure 2 (a) and (b), respectively. The orientation of water has been chosen on the basis of our earlier results using DFT considering

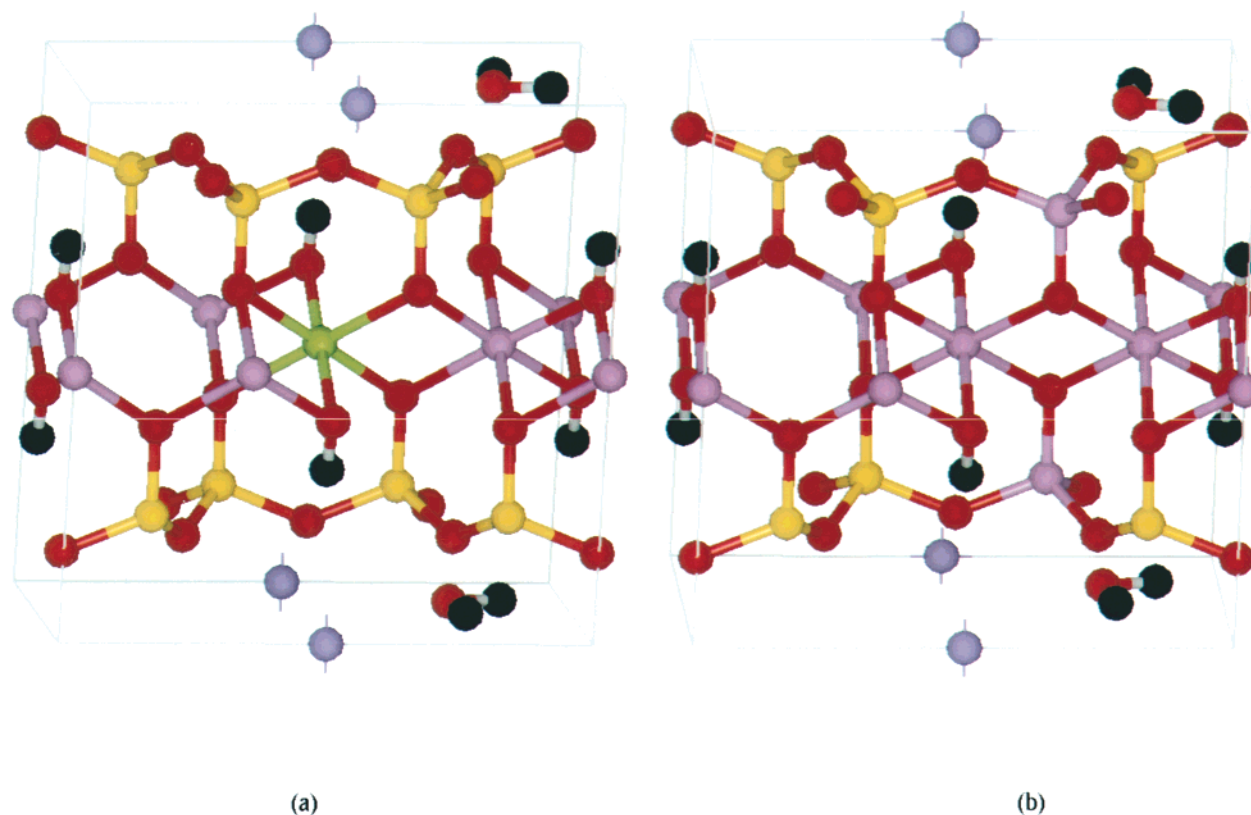


Figure 2. Initial orientation of water molecule with respect to idealized (a) montmorillonite and (b) beidellite projected onto the a - c plane. The color code is as follows: red, oxygen; yellow, silicon; magenta, octahedral aluminum; black, hydroxyl hydrogen; purple, interlayer sodium.

five water molecules surrounding sodium.²³ This is also in agreement with the results of Delville et al.² We observed that among the five, four water molecules lie in the same plane with that of the Na^+ cation and the fifth one is pinched between the cation and the clay surface. As here our aim is to monitor the effect of cation on the orientation of water with respect to clay surface, we have chosen this orientation of the water molecule as the initial orientation. So the water molecule points the lone pair of its oxygen to the Na^+ cation, and it directs one hydrogen toward the center of the cavity while the other is going away from the surface. The location of water minima at the hexagonal hole is known from IR results.⁴⁸ The relaxation of the ions to calculate the minimum energy structures was performed as the following. Unhydrated pyrophyllite structures were minimized using two steps: (1) the tetrahedral layers were allowed to relax where as the octahedral ions were kept fixed, and (2) all the ions were relaxed simultaneously relative to a fixed octahedral ion (magnesium or aluminum) until the total energies are converged. For the hydrated system, as we are using the minimized unhydrated structure, only the water molecule and the hydroxyl group attached to octahedral aluminum were relaxed. We fixed the lattice parameters, i.e., keeping the number of plane waves fixed and allowing the cut-off energy to vary throughout our calculation. This is the best possible way to compromise between computational cost and accuracy.

The $\text{Al}_2\text{Si}_6\text{O}_{24}\text{H}_{18}$ cluster was generated from the clay structure as shown in Figure 3a. The detail is mentioned elsewhere.³¹ It displays the top view of one tetrahedral and one octahedral sheet, showing the hexagonal cavities at the oxygen surface of the silicon layers. The dangling bonds were saturated with hydrogens, not shown in Figure 3a for visual clarity. The hydroxyl group at the center of the hexagonal cavity is parallel to the clay surface and pointing in the direction of the vacancy of the octahedral network. Of the two octahedral aluminums,

one is more stable than the other, as reported in our earlier study.²² Therefore, for the local softness calculations a smaller cluster mimicking the situation with one octahedral connected with four silicon and two hydroxyl groups is generated. This cluster has successfully been used for the study involving interaction of 2:1 dioctahedral smectites with dioxin.²⁹ The dangling bonds are saturated with hydrogens at the nearest neighbor position. The formula of this cluster representing montmorillonite is $\text{AlSi}_4\text{O}_{16}\text{H}_{10}$, whereas that representing beidellite is $\text{AlSi}_3\text{AlO}_{16}\text{H}_{11}$. In the case of beidellite a proton is added with the bridging oxygen between silicon and aluminum tetrahedra to neutralize the charge. These clusters are shown in Figure 3, parts b and c, respectively.

Results and Discussion

Our aim is to rationalize the dependence of layer charge of smectites on water orientation in monohydrate in the presence of interlayer sodium in 2:1 dioctahedral smectites. To study the effect of layer charge we have chosen two types of smectites: (1) montmorillonite, where the layer charge is generated from octahedral substitution, and (2) beidellite, where the layer charge is related with the tetrahedral substitution. We primarily use the localized cluster model to evaluate the values of electrophilic condensed local softness (s_x^+) and condensed Fukui functions (f_x^+) of the individual atoms of the cluster models obtained through the ESP technique at the DFT level shown in Table 1 for both the smectite materials chosen, to locate the active site. Next, on the basis of results obtained from Fukui function calculations, we performed ab initio total energy pseudopotential calculations to study the respective structures to monitor the effect of layer charge on the location of interlayer cation along with the orientation of the water molecule to propose the correlation. On the basis of the two methodologies, we validated

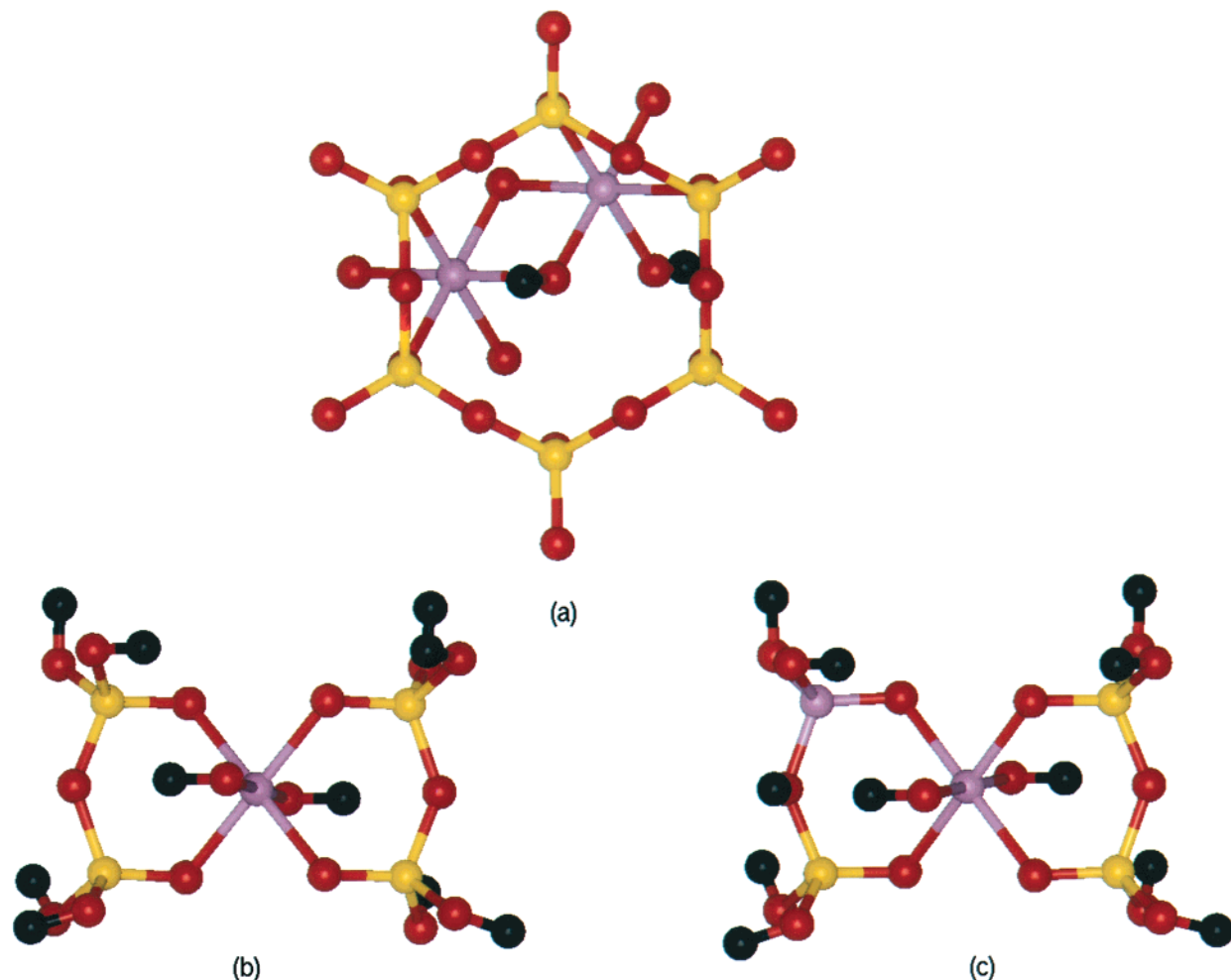


Figure 3. (a) Cluster model of 2:1 dioctahedral clay with six tetrahedral silicons and two octahedral aluminums. It is the top view of the cluster. (b) Initial configuration of a clay cluster having the formula $\text{AlSi}_4\text{O}_{16}\text{H}_{10}$ representing montmorillonite. (c) Initial configuration of a clay cluster having the formula $\text{AlSi}_3\text{AlO}_{16}\text{H}_{11}$ representing beidellite.

the correlation between layer charge and catalytic activity of 2:1 dioctahedral smectites.

a. Reactivity Indexes of the Constituent Atoms of the Representative Clay Clusters for Montmorillonite and Beidellite Using DFT. The aim is to locate the active site in the representative clay structures. The clusters representing idealized montmorillonite and beidellite are shown in Figure 3b,c. As we observed earlier,^{27–29} to test the HSAB principle, it seems that the local softness values, Fukui functions, or reactive indexes of the constituent parameters will be more reliable parameters to look at. Now, here as we have seen that the negative charge originated from the octahedral substitution in case of montmorillonite and from the tetrahedral substitution in case of beidellite, we calculated the local parameters such as Fukui function and local atomic softness for the constituent atoms for the representative clusters. To model the situation of montmorillonite, we substituted the octahedral aluminum of the cluster with Mg^{2+} ; for beidellite the tetrahedral silicon is replaced by Al^{3+} , whereas the aluminum at the octahedral position was kept unperturbed. The results are shown in Table 1. It shows that in case of montmorillonite with Mg^{2+} substitution, the hydroxyl hydrogen attached to the octahedral magnesium acts as the electrophilic site, whereas for beidellite the proton attached to the bridging oxygen between the tetrahedral aluminum and silicon has the highest electrophilicity. This proton has higher electrophilicity in comparison to the hydroxyl hydrogen attached with octahedral aluminum. These results

obtained are somewhat qualitative due to the localized cluster calculation, but it certainly predicts that the active sites present in the smectite structures montmorillonite and beidellite are dependent on the location of substitution in the respective structures. Now, with these results we aim to do a detailed calculation with the *ab initio* total energy pseudopotential method (CASTEP) to rationalize the structure–property relationship.

b. Comparison of Geometric Parameters Using CASTEP. The relative coordinates for idealized montmorillonite and beidellite are calculated and shown in Table 2. The atomic coordinates of pyrophyllite were compared. The results are in good agreement with available experimental values. The deviations are most in case of the basal oxygen atoms of the tetrahedral layer. This is due to rotation of SiO_4 tetrahedra. From the current calculation we observe that SiO_4 is rotated by 13.2° and tilted by 4.6° in average. This is in close agreement with the results obtained by Bridgeman et al.,⁴⁷ whereas for pyrophyllite they observed a rotation of 18.4° and a tilt by 6.5° . The reason for these lies in the fact that in the current study the tetrahedral geometry was not maintained with a reduction of the average $\text{O}_{\text{apex}}\text{—Si—O}_{\text{basal}}$ angle to 108.69° . This results in the increase of Si—O bond length to 1.64 \AA . The average bond lengths for montmorillonite and beidellite are presented in Table 3. In the case of montmorillonite it is observed that the hydroxyl groups is pointed away from the perpendicular, in the direction of the vacancy in the octahedral sheet, making an angle

TABLE 1: Calculated Condensed Local Softness and Fukui Function Values for Clay Clusters with Octahedral and Tetrahedral Substitution by ESP Technique Using DFT

atoms	substituent cation for octahedral Al ³⁺		substituent cation for tetrahedral Si ⁴⁺	
	Mg ²⁺		Al ³⁺	
	f_x^+	s_x^{+a}	f_x^+	s_x^{+b}
Al1	0.150	0.229	0.219	0.487
Si2	0.058	0.089	0.090	0.200
Si3	0.060	0.092	0.077	0.171
Si4/Al2	0.063	0.097	0.132	0.293
Si5	0.053	0.082	0.098	0.218
O6	0.054	0.083	0.091	0.202
O7	0.060	0.092	0.067	0.149
O8	0.064	0.098	0.087	0.193
O9	0.063	0.097	0.088	0.195
O10	0.061	0.093	0.112	0.249
O11	0.051	0.078	0.092	0.204
O12	0.052	0.079	0.087	0.193
O13	0.053	0.081	0.234	0.520
O14	0.057	0.087	0.070	0.155
O15	0.054	0.083	0.076	0.169
O16	0.064	0.098	0.093	0.207
O17	0.061	0.093	0.100	0.222
O18	0.052	0.079	0.093	0.207
O19	0.047	0.073	0.114	0.253
O20	0.402	0.612	0.170	0.378
O21	0.458	0.698	0.187	0.416
H22	0.016	0.025	0.021	0.046
H23	0.012	0.019	0.026	0.057
H24	0.013	0.021	0.003	0.067
H25	0.015	0.024	0.020	0.044
H26	0.013	0.021	0.014	0.031
H27	0.013	0.020	0.020	0.044
H28	0.011	0.018	0.005	0.011
H29	0.011	0.018	0.033	0.073
H30	0.323	0.492	0.168	0.373
H31	0.396	0.603	0.172	0.382
H32			0.302	0.672

^a Global softness for cluster with octahedral substitution = 1.52173 au. ^b Global softness for cluster with tetrahedral substitution = 2.22610 au.

of 24.12° with the a - b plane. This is consistent with the findings of Giese et al.¹⁹ They have shown by minimizing the electrostatic energy of pyrophyllite with respect to the position of the hydroxyl proton, that the OH group made an angle of 26° with the a - b plane. There are no results available to compare with those of beidellite.

c. Location of Interlayer Cation Na⁺ with Respect to the Octahedral Layer Using CASTEP. A generally recognized explanation of the long-range swelling in the clays is the electrostatic repulsion between the clay sheets bearing the same charge. This view is partial since it neglects the contribution of interlayer cations. One must treat the system formed by the charged surface plus the counterions as a whole. The system is neutral and ionic. So here in the current investigation we aim to find the location of the interlayer cation and probe its dependence on the charge resulting from the octahedral/tetrahedral substitution, depending on the structure of the respective clay. In the current investigation we are using two different smectite structures: (1) montmorillonite and (2) beidellite. Now, in montmorillonite one of the octahedral aluminums is substituted by magnesium, which results in the negative charge being neutralized by the interlayer cation (here Na⁺). Here we have monitored the location of Na⁺ in the interlayer by relaxing the Na⁺ cation with the rest of the lattice being kept constant. The results are shown in Figure 4. We plotted the relative stabilization energy of Na⁺ with varying

TABLE 2: Comparison of Internal Coordinates of the 2:1 Dioctahedral Clays

atoms	pyrophyllite			montmorillonite			beidellite		
	x	y	z	x	y	z	x	y	z
Al	0.000	0.008	0.499	-0.000	0.006	0.500	-0.001	0.011	0.497
Al	0.000	0.675	0.500	-0.000	0.672	0.499	-0.006	0.674	0.499
Al	0.500	0.509	0.499	0.499	0.167	0.500	0.496	0.503	0.496
Al/Mg	0.500	0.175	0.500	0.499	0.507	0.499	0.497	0.178	0.494
O	0.014	-0.000	0.161	0.075	0.000	0.149	0.002	0.002	0.165
O	0.985	0.001	0.838	0.925	0.000	0.851	0.971	-0.003	0.842
O	0.666	0.037	0.397	0.686	0.030	0.393	0.669	0.037	0.399
O	0.334	0.037	0.602	0.312	0.030	0.606	0.324	0.042	0.604
O	0.513	0.497	0.161	0.586	0.500	0.151	0.495	0.511	0.150
O	0.486	0.499	0.838	0.413	0.500	0.847	0.468	0.496	0.840
O	0.326	0.227	0.160	0.373	0.238	0.145	0.358	0.208	0.149
O	0.674	0.229	0.840	0.626	0.238	0.854	0.657	0.227	0.842
O	0.679	0.768	0.815	0.611	0.776	0.831	0.645	0.772	0.817
O	0.319	0.766	0.184	0.388	0.776	0.168	0.352	0.787	0.188
O	0.805	0.735	0.156	0.879	0.730	0.142	0.846	0.723	0.161
O	0.193	0.736	0.842	0.119	0.730	0.857	0.154	0.720	0.843
O	0.160	0.276	0.811	0.107	0.275	0.834	0.142	0.277	0.821
O	0.839	0.275	0.188	0.891	0.275	0.165	0.893	0.297	0.173
O	0.161	0.149	0.390	0.180	0.148	0.385	0.163	0.152	0.386
O	0.838	0.150	0.609	0.818	0.148	0.615	0.834	0.150	0.612
O	0.935	0.841	0.612	0.902	0.844	0.614	0.919	0.841	0.612
O	0.064	0.841	0.387	0.096	0.844	0.385	0.075	0.840	0.392
O	0.654	0.651	0.389	0.686	0.663	0.385	0.658	0.649	0.389
O	0.345	0.651	0.610	0.312	0.663	0.614	0.330	0.650	0.609
O	0.425	0.342	0.610	0.384	0.324	0.613	0.410	0.341	0.612
O	0.574	0.341	0.389	0.614	0.324	0.386	0.581	0.342	0.394
O	0.164	0.537	0.397	0.160	0.546	0.374	0.157	0.531	0.399
O	0.835	0.537	0.602	0.839	0.547	0.625	0.824	0.537	0.607
H	0.571	-0.039	0.341	0.612	-0.052	0.337	0.601	-0.006	0.311
H	0.428	-0.039	0.658	0.387	-0.053	0.662	0.412	-0.033	0.663
H	0.068	0.457	0.346	0.063	0.469	0.322	0.063	0.443	0.361
H	0.931	0.458	0.653	0.937	0.469	0.677	0.922	0.449	0.642
Si/Al	0.081	0.162	0.223	0.128	0.163	0.213	0.588	0.334	0.216
Si	0.918	0.164	0.776	0.871	0.163	0.786	0.104	0.167	0.216
Si	0.946	0.835	0.778	0.888	0.834	0.786	0.904	0.159	0.778
Si	0.052	0.833	0.221	0.111	0.834	0.213	0.920	0.831	0.778
Si	0.569	0.662	0.222	0.625	0.668	0.216	0.072	0.838	0.225
Si	0.430	0.663	0.777	0.374	0.668	0.783	0.584	0.666	0.222
Si	0.434	0.334	0.776	0.383	0.331	0.782	0.404	0.660	0.774
Si	0.565	0.333	0.223	0.616	0.331	0.217	0.418	0.331	0.777
Na				0.997	0.487	-0.001	1.067	0.480	0.024

TABLE 3: Comparison of Average Bond Lengths of 2:1 Dioctahedral Smectite

bond	bond length (Å)		
	pyrophyllite	montmorillonite	beidellite
O _{basal} -O _{basal}	2.66	2.68	2.64
O _{basal} -O _{apex}	2.65	2.65	2.64
O _{basal} -Si	1.64	1.64	1.62
O _{apex} -Si	1.64	1.62	-
O _{apex} -Al	-	-	1.71
O-Mg/Al	1.92	1.92	1.94
O-O(oct)	2.68	2.67	2.64
O-H	0.97	0.97	0.97

Na-Mg distance. The final geometry shows that Na⁺ has a tendency to go nearest to the Mg²⁺ cation, as expected and proposed in our earlier study with localized cluster models.²³ At the stablest configuration the Na-Mg distance is 3.5 Å. Now the results for the dependence of tetrahedral aluminum in binding the interlayer cation Na⁺ are plotted in Figure 5. The results show that the optimum Na-Al distance is 2.8 Å for beidellite. The result also validates the proposition of active site obtained from Fukui function calculations. This result is also in perfect match with the experimental observation supported by Monte Carlo calculation that Na⁺ has a strong tendency to lie close to clay sheets in the case of tetrahedral substitution. Now the things which can be proposed at this point of calculation are the following:(1) in beidellite, the tetrahedral Al³⁺ has a more pronounced role than that of montmorillonite; (2) in mont-

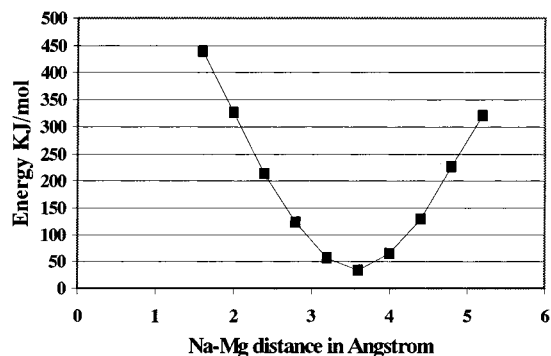


Figure 4. Potential energy curve for the optimum distance between interlayer sodium and octahedral magnesium in montmorillonite.

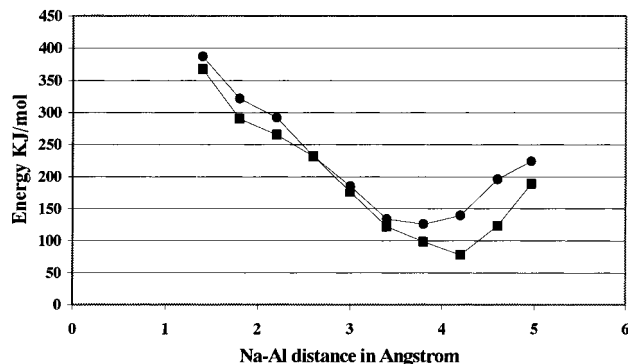


Figure 5. Potential energy curve for the optimum distance between interlayer sodium and tetrahedral aluminum in beidellite.

morillonite, the Mg^{2+} is the cation in the octahedral layer with which the Na^+ has a favorable interaction; and (3) in beidellite, the cation resides closer to the clay surface.

These results are in perfect agreement with the MD results of Teppen et al.¹⁰ They have shown that d spacing of Na-beidellite tends to be smaller than that of Na-smectites, as most of their structural charges resides in the tetrahedral sheet causing stronger interlayer electrostatic forces.

d. Orientation of Water with Respect to the Hydroxyl Proton Attached with Octahedral Aluminum by CASTEP. Most of the catalytic properties of clay are due to its acidic character, which is significantly influenced by the clay structure. Upon calcination of octahedrally substituted smectites (e.g., montmorillonite) protons can migrate into vacancies in the octahedral sheet where they are bound to structural oxygens. The migrated protons are no longer available for catalytic reactions. The remaining acid sites are mainly of the Lewis type. In tetrahedrally substituted smectites (e.g., beidellite), however, the protons are attached to surface oxygens of the tetrahedral sheet. These Bronsted sites are similar to those within Y-zeolite.⁴⁹ Here our aim is to trace the orientation and location of the water molecule with respect to the hydroxyl hydrogen attached to the octahedral aluminum. Hence, we kept the framework lattice constant and optimized the water molecule at various distances with the water lying parallel to the clay surface with one of its hydrogens keeping away from the framework. The initial configuration of the water molecule is shown in Figure 2a. The stabilization energy with respect to the distance between oxygen of water and hydrogen of hydroxyl proton are plotted in Figure 6. The results show that in case of montmorillonite the interaction probability between water and the hydroxyl hydrogen attached to the octahedral site is maximum at a distance of 3.5 Å. In beidellite, the interaction probability using its hydroxyl hydrogens attached with the

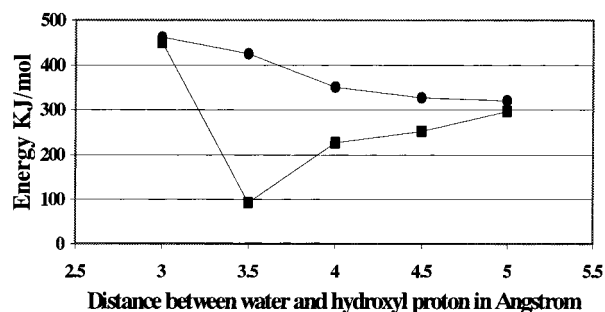


Figure 6. Potential energy curve to study the feasibility of formation of H_3O^+ in terms of the distance between water oxygen and hydroxyl proton attached to octahedral site in both montmorillonite (■) and beidellite (●).

octahedral aluminum is remote. This is obvious, as in case of montmorillonite the hydroxyl hydrogen is attached with a lesser charge moiety Mg^{2+} which influences the activity of hydroxyl hydrogen, as observed from the Fukui function results. Now, from IR studies⁴⁸ it is observed that the water molecule indeed can form the hydrogen bond with the lone pair of the oxygen at the center of the cavity. This is possible for dioctahedral clays since the proton is directed parallel to the plane of the clay. Here we have only considered the interaction between the water and the hydroxyl proton influenced by the octahedral layer. In beidellite, charge imbalance results from the substitution on the tetrahedral layer, so here comes the need for monitoring the interaction of water with surface oxygen.

e. Orientation of Water with Respect to the Surface Oxygen Using CASTEP. The Monte Carlo simulation performed by Chang et al.^{50,51} has indicated that Na^+ counterions form the inner sphere surface complex with siloxane surface oxygen near sites of isomorphic substitution in the tetrahedral sheet of Na-smectite, whereas in the one layer hydrate the Na^+ form outersphere surface complexes with siloxane surface oxygen near sites of isomorphic substitution in the octahedral sheet. Prost et al.⁹ have proposed that in case of smectites which have their isomorphic substitution in the tetrahedral site sheet, water molecules adsorbed in the interlamellar spaces are involved in hydrogen bonding with oxygen atoms belonging to tetrahedral SiO_4^- replaced by AlO_4^- tetrahedra. From the Fukui function calculations we observed that the proton attached with the substituted tetrahedral aluminum bridged oxygen is the active site. Now, the hydrogen atoms of water molecules may be attracted to the negative charge generated due to the substitution of tetrahedral silicon by aluminum; this may result in the interaction of water hydrogens with the hydrogen of the surface hydroxyl group paving the formation of H_3O^+ . So here we aim to monitor the probability of surface interaction between the water and the surface oxygen for both montmorillonite and beidellite. The initial model of water orientation in case of beidellite is shown in Figure 2b. In the case of montmorillonite, this initial configuration is the same with a difference only in the octahedral sheet, with one of the aluminums is replaced by Mg^{2+} . We kept fixed the framework lattice and optimized the water with varying distances from the surface. The results are shown in Figure 7. The results show that the surface interaction is a more feasible process in the case of beidellite in comparison to that of montmorillonite when the surface hydrogens are involved. In case of beidellite the negative charge is generated on the surface due to the substitution of surface SiO_4^- by AlO_4^- ; this paves the way for the surface interaction. Whereas, in case of montmorillonite the negative center is located down in the octahedral sheet so the surface interaction does not occur. Here the sodium has practically negligible influence in the surface

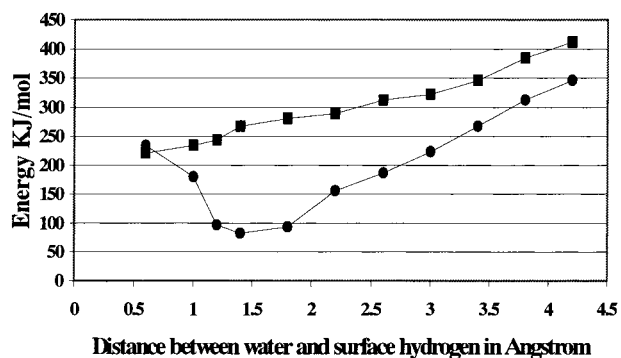


Figure 7. Potential energy curve to study the feasibility of hydrogen-bond formation over the clay surface in terms of the distance between water oxygen and surface hydrogen in both montmorillonite (■) and beidellite (●).

interaction. As the results show that hydrogen bonding probability is maximum at a distance of 1.4 Å between water and surface. These results show that the location of layer charge is detrimental on binding the interlayer cation along with the water molecule. Now the water surface interaction is favored with surface when tetrahedral substitution is present, while interaction of water with hydroxyl hydrogen attached with the octahedral site is favored when the layer charge originates from octahedral substitution. These interactions are not influenced by the presence of sodium. Now during hydration when a few more water molecules approach the interlayer cation then hydration effect comes into play. This hydration is influenced by the nature and number of cations present in the unit cell. In the current study, sodium has a favorable interaction with the oxygen of a single water resulting in an energetically stable conformer. The discontinuous model for adsorbed water, i.e., to say the presence of two kinds of water molecules, one corresponding to water molecules which hydrate the exchangeable cation and the second adsorbed on the surface is supported by experiment performed in the near-IR range.⁵² The current study involves a single water molecule so the influence of sodium is not well traced; this needs further calculation in the presence of a greater number of water molecules to follow the hydration. This is the aim of our next study using ab initio molecular dynamics method.

These results clearly indicate the role of layer charge in governing the location of interlayer cation and as well as the water molecule surrounding the interlayer cation. These optimistic results pave the way to correlate the relative humidity with the number of water layers present in the interlayer, which dictates the important swelling phenomenon for clay.

Conclusion

This is the first study to correlate the layer charge with the catalytic activity of the 2:1 dioctahedral smectite. In the present study our aim was first to locate the active site of the individual clay structures and to find whether it has any business with the layer charge at all. With the local Fukui function and local atomic softness values within the helm of DFT we were successful in showing that the layer charge plays a key role in determining the active site of the clay structure. Next we wished to locate the optimized position of the interlayer cation with respect to the clay sheet. For doing this we have chosen the best available periodic calculation methodology—the ab initio total energy pseudopotential method (CASTEP). This method is used to explore the lattice structure in a nice way. These helps further to get rid of the approximations involved in cluster calculations and is also useful to monitor the effect of a

particular constituent over the whole structure. It is observed that the interlayer cation Na^+ stays close to the site of isomorphous substitution. Second, we monitored the feasibility of formation of hydrogen bonding with the bridging hydroxyl attached to octahedral cation. It is observed that the formation is smooth in the case of montmorillonite, but in case of beidellite it is forbidden. The reason behind this is the presence of isomorphous substitution in the octahedral layer in case of montmorillonite. This was followed by the study to monitor the feasibility of surface hydrogen bonding which is possible due to the isomorphous substitution occurring at the tetrahedral layer of beidellite. Interestingly enough, the results show that surface hydrogen-bonding is favored in the case of beidellite. The results show that for a single water molecule the influence of sodium is negligible. Now we explored the correlation in two representative structures of 2:1 dioctahedral smectite: one has a tetrahedral substitution, and another has an octahedral one. So these results can be extrapolated to all the constituent members of the 2:1 dioctahedral family to validate the correlation. The effect of sodium needs further calculation in the presence of a greater number of water molecules. The successful prediction of the location of interlayer cation and the orientation of the water molecules in the interlayer are encouraging and indicate that total energy pseudopotential calculations may prove a useful technique to assist future experimentation. Now here we first predicted the location of active sites by Fukui function results, which is further validated by periodic ab initio calculations. This is the novelty in terms of methodology. We therefore can extrapolate this kind of correlation for other complicated structures. The optimistic results pave the way for our future calculation to correlate humidity with layer charge which will guide us to formulate an a priori rule for the swelling of smectite clays.

References and Notes

- (1) Sposito, G.; Prost, R. *Chem. Rev.* **1982**, *82*, 553.
- (2) Delville, A. *Langmuir* **1991**, *7*, 547.
- (3) Sposito, G.; Prost, R. *Chem. Rev.* **1982**, *82*, 554.
- (4) Laird, D. A. *Clays Clay Miner.* **1996**, *44*, 553.
- (5) Newman, A. C. D. In *Chemistry of Clays and Clay Minerals*; Newman, A. C. D., Ed.; Wiley: New York, 1987; pp 1–128.
- (6) Guven, N. In *Clay-Water Interface and Its Rheological Implications*; Guven, N., Pollastro, R. M., Eds.; The Clay Mineral Society: Boulder, 1992; pp 2–79.
- (7) Aliosi, G.; Foresti, M. L.; Guidelli, R.; Barnes, P. *J. Chem. Phys.* **1989**, *91*, 5592.
- (8) Skipper, N. T. *Mineral. Mag.* **1998**, *62*, 657.
- (9) Prost, R.; Koutit, A.; Benchara, A.; Huard, E. *Clays Miner.* **1998**, *46*, 117.
- (10) Teppen, B. J.; Rasmussen, K.; Bertsch, P. M.; Miller, D. M.; Schafer, L. *J. Phys. Chem. B* **1997**, *101*, 1579.
- (11) Shroll, R. M.; Smith, D. E. *J. Chem. Phys.* **1999**, *111*, 9025.
- (12) Kutter, S.; Hansen, J. P.; Sprik, M.; Boek, S. *J. Chem. Phys.* **2000**, *112*, 311.
- (13) Delville, A. *J. Phys. Chem.* **1995**, *99*, 2033.
- (14) Boek, E. S.; Coveney, P. V.; Skipper, N. T. *J. Am. Chem. Soc.* **1995**, *117*, 12608.
- (15) Chang, F. R. C.; Skipper, N. T.; Sposito, G. *Langmuir* **1998**, *14*, 1201.
- (16) Sposito, G.; Park, S. H.; Sutton, R. *Clays Clay Miner.* **1999**, *47*, 192.
- (17) Boek, E. S.; Coveney, P. V.; Skipper, N. T. *Langmuir* **1995**, *11*, 4629.
- (18) Laird, D. A. *Clays Clay Miner.* **1999**, *47*, 630.
- (19) Giese, R. F. *Nature* **1973**, *241*, 151.
- (20) Ebina, T.; Iwasaki, T.; Chatterjee, A.; Katagiri, M.; Stucky, G. D. *J. Phys. Chem. B* **1997**, *101*, 1125.
- (21) Chatterjee, A.; Iwasaki, T.; Ebina, T.; Hayashi, H. *Appl. Surf. Sci.* **1997**, *121/122*, 167.
- (22) Chatterjee, A.; Iwasaki, T.; Hayashi, H.; Ebina, T.; Torii, K. *J. Mol. Catal. A* **1998**, *136*, 195.
- (23) Chatterjee, A.; Iwasaki, T.; Ebina, T.; Miyamoto, A. *Comput. Mater. Sci.* **1999**, *14*, 119.
- (24) Pearson, R. G. *J. Am. Chem. Soc.* **1983**, *105*, 7512.

- (25) Pearson, R. G. *J. Chem. Educ.* **1987**, *64*, 561.
(26) Parr, R. G.; Yang, W. *J. Am. Chem. Soc.* **1984**, *106*, 4049.
(27) Chatterjee, A.; Iwasaki, T.; Ebina, T. *J. Phys. Chem. A* **1999**, *103*, 2489.
(28) Chatterjee, A.; Iwasaki, T. *J. Phys. Chem. A* **1999**, *103*, 9857.
(29) Chatterjee, A.; Iwasaki, T.; Ebina, T. *J. Phys. Chem. A* **2000**, *104*, 2098.
(30) Kohn, W.; Sham, L. J. *Phys. Rev. A* **1965**, *140*, 1133.
(31) Becke, A. J. *J. Chem. Phys.* **1988**, *88*, 2547.
(32) Lee, C.; Yang, W.; Parr, R. G. *Phys. Rev. B* **1988**, *37*, 786.
(33) Bock, C. W.; Trachtman, M. *J. Phys. Chem.* **1994**, *98*, 95.
(34) Proft, F. D.; Martin, J. M. L.; Geerlings, P. *Chem. Phys. Lett.* **1996**, *250*, 393.
(35) Teter, M. P.; Payne, M. C.; Allen, D. C. *Phys. Rev. B* **1989**, *40*, 12255.
(36) Payne, M. C.; Teter, M. P.; Allan, D. C.; Arias, T. A.; Johannopoulos, J. D. *Rev. Mod. Phys.* **1992**, *64*, 1045.
(37) Perdew, J.; Zunger, A. *Phys. Rev. B* **1981**, *23*, 5048.
(38) Winkler, B.; Milman, V.; Payne, M. C. *Am. Mineral.* **1994**, *79*, 200.
(39) Perdew, J. P. *Phys. Rev. B* **1986**, *33*, 8822.
(40) Becke, A. D. *Phys. Rev. A* **1988**, *33*, 3098.
(41) Laasonen, K.; Csajka, F.; Parrinello, M. *Chem. Phys. Lett.* **1992**, *194*, 172.
(42) Lee, C.; Vanderbilt, D.; Laasonen, K.; Car, R.; Parrinello, M. *Phys. Rev. B* **1993**, *47*, 4863.
(43) Garcia, A.; Elsasser, C.; Zhu, J.; Louie, S. G.; Cohen, M. L. *Phys. Rev. B* **1992**, *46*, 9829.
(44) Monkhorst, H. J.; Pack, J. D. *Phys. Rev. B* **1976**, *13*, 5188.
(45) Newman, A. C. D.; Brown, G. In *Mineralogical Society Monograph No. 5, Chemistry of Clays and Clay Minerals*; Newman, A. C. D., Ed.; Mineralogical Society: London, 1974; p 10.
(46) Lee, J. H.; Guggenheim, S. *Am. Mineral.* **1981**, *66*, 350.
(47) Bridgeman, C. H.; Buckingham, A. D.; Skipper, N. T.; Pyne, M. C. *Mol. Phys.* **1996**, *89*, 879.
(48) Sposito, G.; Prost, R. *Chem. Rev.* **1982**, *82*, 553.
(49) Barrer, R. M. In *Zeolite and Clay Materials as Sorbents and Molecular Sieves*; Academic Press: New York, 1978.
(50) Chang, F. R. C.; Skipper, N. T.; Sposito, G. *Langmuir* **1995**, *11*, 2734.
(51) Chang, F. R. C.; Skipper, N. T.; Sposito, G. *Langmuir* **1995**, *13*, 2074.
(52) Luck, W. A. P. In *Water: A comprehensive treatise. Water in crystalline hydrates. Aqueous solution of simple nonelectrolytes*; Plenum Press: New York, 1973; pp 235–321.